

Author Query Form

Journal : Journal of Earthquake Engineering

Articleid: 223185

Dear Author,

During the copy-editing of your paper, the following queries arose. Please respond to these by marking up your proofs with the necessary changes/additions. Please write your answers on the query sheet if there is insufficient space on the page proofs. If returning the proof by fax do not write too close to the paper's edge. Please remember that illegible mark-ups may delay publication.

Many thanks for your assistance.

Ref. no:	Query	Remarks
1	Au: City: ?	
2	Au: book title?	
3	Au: Editors of book? Pls. provide 1st initials	
4	AU: Pls. provide RRH.	

Site Classification Assessment for Estimating Empirical Attenuation Relationships for Central-Northern Italy Earthquakes

M. MASSA, S. MARZORATI, E. D'ALEMA, D. DI GIACOMO,
and P. AUGLIERA

5

Istituto Nazionale di Geofisica e Vulcanologia, Milano, Italy

The aim of this article is to investigate the ground motion attenuation of the most industrialized and populated regions of Italy, evaluating the capability of different approaches to estimate site dependent models. The 5.2 magnitude earthquake on November 24, 2004 shocked the areas of Northern Italy producing damage of about 215 million euros. The data set, including 243 earthquakes of local magnitude up to 5.2, has been collected in the period December 2002–October 2005 by 30 three-component seismic stations managed by Istituto Nazionale di Geofisica e Vulcanologia, Sezione of Milano (INGV-MI). Empirical attenuation relationships have been estimated for horizontal peak ground velocity (PGHV), acceleration (PGHA), displacement (PGHD), and for response spectral acceleration (SA) for periods between 0.1 and 1.5 s. To estimate suitable attenuation models, in particular for sites characterized by thick sedimentary geological formations, a soil discrimination based on EU8 code can lead to wrong evaluations. On the contrary, a classification based on H/V spectral ratios of seismic ambient noise (NHV) allows the models to fit better real and predicted data and to reduce the uncertainties of the process. For each receiver, NHV have been strengthened by additional H/V spectral ratio of earthquake data (EHV), calculated considering different portions of the analysed signals. In order to validate the PGHA attenuation relationship for greater magnitudes, accelerometric records, relative to Central-Northern Italy strong motions occurring in the last 30 years, have been collected and superimposed to our attenuation curves.

Keywords Attenuation; Waveform Analyses; H/V Spectral Ratio

1. Introduction

25

The estimate of reliable ground motion attenuation relationships represents one of the most important tasks in seismic hazard assessment [Cornell, 1968]. The most common method to evaluate seismic hazard, related to ground shaking, is to make use of predictive ground motion models. The empirical attenuation relationships are usually models expressed as mathematical functions relating the ground motion parameters to the source properties, the propagation medium and the local site geology. In the last years, several studies concerning the ground motion attenuation relationships have been accomplished; nowadays, many predictive equations, estimated from strong motion recordings, are available both for Italian regions [Bindi *et al.*, 2006, from the Umbria-Marche earthquakes; Bragato and Slejko, 2005, from the Eastern Alps earthquakes; Sabetta and Pugliese, 1987, 1996, from the Italian earthquakes] and for wider regions [e.g., Ambraseys *et al.*, 1996 a,b, 2005 a,b, from Europe earthquakes; Atkinson and Boore, 1997, from Eastern North

Received 23 March 2006; accepted 11 January 2007.

Address correspondence to M. Massa, Istituto Nazionale di Geofisica e Vulcanologia, Sezione di Milano, via Bassini 15, 20133 Milano, Italy; E-mail: massa@mi.ingv.it

America earthquakes; Boore *et al.*, 1993, 1994, from Western North America earthquakes; Campbell, 1985, 1997, from both North America and worldwide earthquakes; Sadig *et al.*, 45 1997, from Western North America earthquakes; Toro *et al.*, 1997, from Eastern and Central North America earthquakes]. Although almost all the attenuation relations are calibrated using strong motion data, the non negligible weight of low magnitude events on seismic hazard evaluation has also been recognized [Reiter, 1990]. In particular, for industrial and highly populated areas, as pointed out by Campbell [1989], small events may be 50 of interest from an engineering point of view; indeed, even if they do not produce peak ground acceleration able to compromise well-engineered structures, they can compromise more sensitive components, such as mechanical and electrical equipment of industrial plants. This consideration leads to the conclusion that well-calibrated attenuation relationships, spanning from weak motions [Campbell, 1989, from Eastern North America earthquakes; Costa *et al.*, 1998, from Friuli earthquakes; Theodulidis, 1998, from Greece earthquakes; Frisenda *et al.*, 2005, from North-Western Italy earthquakes; Dost *et al.*, 55 2004, from Netherlands earthquakes] to strong motions, are necessary. The calibration of regional attenuation relationships represents an important assessment in order both to compile seismic hazard map at local scale (often requested by public administration) and 60 to estimate shaking scenarios relative to a particular source, especially in the case in which no records are available in the near field. Furthermore, the influence of regional crustal structures on the ground motion, in particular in the middle and in the far-field (distances greater than 50 km), has been demonstrated [Suhadolc and Chiaruttini, 1987]. In this article the ground motion attenuation of the most populated and industrial areas of Central- 65 Northern Italy has been investigated analyzing a data set composed both of weak and strong motion recordings (Fig. 1a). In this area the attenuation characteristics are largely unknown due both to low seismicity and to the lack (for the past) of instrumental coverage. Moderate seismic events, occurring in this area in the last years (i.e., November 25, 2004 Salò earthquake, $M_I=5.2$; September 14, 2003 Monghidoro earthquake, $M_I=5.0$; 70 April 11, 2003 Novi Ligure earthquake, $M_I=4.7$; August 21, 2000 Acqui Terme earthquake, $M_I=5.1$, URL: www.ingv.it), document and confirm the presence of a non negligible seismic activity. In particular, the November 25, 2004 Salò earthquake ($M_I=5.2$) has been the strongest event to shock the Lombardia region in the last decades. On the basis of the official data provided by the Lombardia Region authorities, this earthquake, felt on the 75 whole North-Italy area, strongly affected 66 municipalities close to the epicentral area, damaging about 3,700 buildings (involving about 2,500 people) and 300 churches, for an approximate damage evaluation of 215 million euros. It is worth noting that in the past the area under study was shocked by several energetic events such as the October 30, 1901 Salò earthquake ($I_0=VIII$ MCS; Camassi and Stucchi, 1996). At present, for the area 80 under study, only attenuation relationships (for frequencies ranging from 1.0–20 Hz) estimated by Castro *et al.* [1993], based on six earthquakes with magnitude ranging from 2.5–3.6 and hypocentral distances between 23 and 125 km, are available. The results reported in the seismic hazard map of Italy [Gruppo di lavoro, 2004] show that the area under study appears to be characterized by predictable horizontal acceleration peaks ranging from 85 0.150–0.175 g. These results have been obtained by applying the Ambraseys *et al.* [1996 a,b] and Sabetta and Pugliese [1996] empirical PGHA attenuation relationships. In this article the attenuation curves, calculated for peak ground accelerations (PGHA), velocities (PGHV), displacements (PGHD), and spectral accelerations (SA), have been estimated starting from a data set including 243 local earthquakes (about 3,500 waveforms) of local 90 magnitude ranging from 2.5–5.2, occurring in the period of December 2002–October 2005. The regressions, performed in order to obtain both site and no site dependent ground motion prediction equations, have been implemented by using a simple model, function of

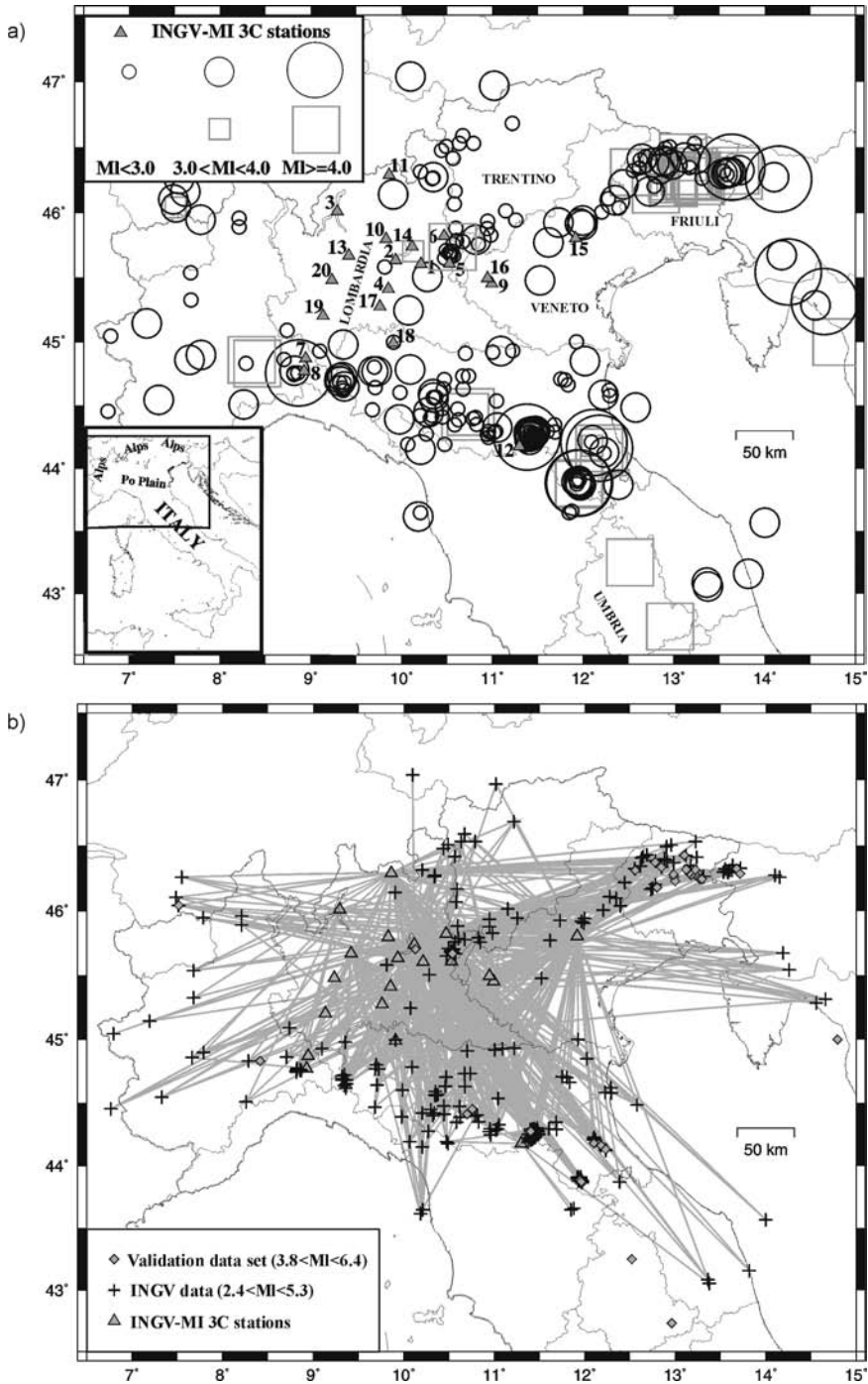


FIGURE 1 Map showing the locations of the seismic events (black circles) recorded by INGV-MI stations (grey triangles) in the period December 2002–October 2005. The epicentral coordinates of all strong motions used as comparison (grey squares), and reported in Table 2, are also shown. b) Ray paths between the events included in the dataset (black crosses) and the INGV-MI 3C stations.

magnitude, distances and site geology, and considering weak and strong motion recordings characterized by hypocentral distances up to 300 km. The evaluation of site coefficients has been performed both by following the site classification reported in the EU8 code [ENV, 2002] and by evaluating the site response using simple NHV [Nakamura, 1989] and EHV analysis.

2. Data and Data Processing

Since December 2002, the seismicity of the study area (longitude ranging from about 9°E to 12°E50' and latitude ranging from about 44°N to 46°N) has been continuously monitored by 30 velocimetric stations (working in different periods) installed, as showed in Fig. 1a, in 20 different sites. In the past, this area was poorly monitored: at the end of 2002 the Lombardia Region was covered by only 3 RSNC (National Centralized Seismic Network, URL: www.ingv.it) velocimetric stations and one RAN (National Accelerometric Network, URL: www.protezionecivile.it) accelerometric station, all equipped with vertical sensors. At present, the INGV-MI network (Fig. 1a) consists of 9 digital three-component seismometers (equipped with 4 Nanometrics Trillium 40, with flat response between 0.025 and 50 Hz, 4 Lennartz LE3D-5s, with a flat response between 0.2 and 40 Hz, and 1 Lennartz LE3D-lite with a flat response between 1 and 80 Hz) located in the core of the area of interest. Starting from May 2005 the network has been further developed by the installation of three Kinematics-Episor accelerometers in the sites indicated in Fig. 1a by numbers 14, 19, and 20. The sensors are coupled both with Lennartz Mars88-MC (URL: www.lennartzelectronic.de) and Reftek 130 (URL: www.reftek.com). The data acquisition has been performed at a sampling rate of 62.5 samples/sec, so that a minimum antialias cutoff of 25 Hz has been guaranteed. The main features of all seismic stations are reported in Table 1. The epicenters of the events used in this study to calibrate the attenuation relationships are shown in Fig. 1a. In order to calculate reliable focal coordinates, the arrival times of the events recorded by INGV-MI network (in particular related to the great amount of weak motions occurred in the study area) have been added to the information coming from the INGV-CNT data set, so that all earthquakes have been re-localized. The data have been selected a priori on the basis of local magnitude, in order to discard the events characterized by $M_l < 2.5$, and hypocentral distances greater than 300 km. The local magnitude is calculated using an M_l scale calibrated for Central-Northern Italy region by Augliera *et al.* [2004], following the approach proposed by Spallarossa *et al.* [2002]. In Figs. 1b and 2, the source-stations ray-paths and the distribution of the recordings versus distance (for different magnitudes) are shown. In the same figures the information related to the strong motions, occurred in Central-Northern Italy in the last 30 years and used as comparison (see Table 2) are also reported. The small number of earthquakes with M_l values greater than 4.0, and in particular greater than 5.0, are a consequence of the intrinsic characteristics of the North Italy seismicity. The seismic events characterized by $M_l < 4.0$ ensure a completeness of information for all distances (0–300 km), whereas at short distances there are few recordings for events of $M_l > 4.0$. In order to reduce the natural noise only the recordings characterized by a signal to noise ratio greater than 10 dB have been selected. The final outcome is a data set composed of 2,126 high-quality horizontal velocimetric waveforms, recorded between December 2002 and October 2005, related to 243 earthquakes with local magnitude spanning from 2.5–5.2 and hypocentral distances up to 300 km. Starting from the selected signals both peak ground horizontal accelerations and peak ground horizontal displacements have been obtained. The waveforms have been a priori base-line corrected, the effect of the instrument response removed and band pass filtered between 0.5–25 Hz; finally, the velocimetric signals have

TABLE 1 Description of the stations considered in this study. The grey cells indicate the INGV-MI stations working nowadays

ID	Station code	Site	Lat (°)	Long (°)	Elevation (m)	Installation data	Removal data	Rec (H) x2	Sensor	EU8 soil category	H/V noise (mean 0.1-1 s)	H/V quakes (mean 0.1-1 s)	Coeff. Site Effect	Dummy	Mag residuals
1	M155	Concesio	45.6062	10.2155	210	12/05/02	03/11/03	18	Mark L4-3D	C	-	-	-	1	0.20
2	M161	Capriolo	45.6375	9.9338	253	12/16/02	03/12/03	17	Mark L4-3D	B	-	-	0	0	-0.15
3	M150	Perledo	46.0107	9.2910	219	02/18/03	05/27/03	54	Mark L4-3D	A	1.12	1.28	0	0	-0.31
4	SONC	Soncino	45.4123	9.8554	90	03/06/03	06/30/04	34	Mark L4-3D	B	-	-	-	1	+0.074
5	M152	Salò	45.6080	10.5260	123	02/27/03	03/11/03	13	Mark L4-3D	B	-	-	-	1	+0.073
6	BAG3	Bagolino	45.8228	10.4664	807	09/16/04	05/12/03	60	LE-3D/5sec	A	1.40	1.43	0	0	-0.12
6	BAG0	Bagolino	45.8217	10.4678	767	03/12/03	05/12/03	14	Mark L4-3D	A	1.40	1.43	0	0	-0.12
6	BAG2	Bagolino	45.8228	10.4664	807	05/12/03	09/16/04	118	Mark L4-3D	A	1.40	1.43	0	0	-0.12
7	SARE	Sarezzano	44.8705	8.9429	284	05/13/03	05/20/03	8	Mark L4-3D	A	-	-	0	0	-0.010
8	SARD	Sardigliano	44.7707	8.9276	340	06/05/03	06/11/03	8	Mark L4-3D	A	-	-	0	0	-0.007
9	VER2	Verona	45.3970	10.9609	174	11/26/03	06/29/04	5	Mark L4-3D	A	1.32	1.65	0	0	-0.016
9	VER0	Verona	45.4546	10.9941	174	06/17/03	11/26/03	46	Mark L4-3D	A	1.32	1.65	0	0	-0.016
10	GAZZ	Gazzaniga	45.7986	9.8290	475	07/15/03	10/14/03	15	Mark L4-3D	A	-	-	1	1	+0.040
11	MAL3	Malenco	46.2918	9.8636	2030	07/15/04	09/04/03	28	LE-3D/5sec	A	1.61	1.88	1	1	+0.028
11	MAL0	Malenco	46.2914	9.8650	2030	03/14/03	09/04/03	22	Mark L4-3D	A	1.61	1.88	1	1	+0.028
11	MAL2	Malenco	46.2918	9.8636	2030	07/28/03	07/15/04	49	Mark L4-3D	A	1.61	1.88	1	1	+0.028
12	OGGI	Monghidoro	44.1773	11.2988	970	09/15/03	10/28/03	35	Mark L4-3D	A	-	-	1	1	+0.34
13	MER2	Merate	45.6725	9.4182	350	05/03/04	10/28/03	32	Trillium	B	2.03	1.41	1	1	+0.16
13	MER0	Merate	45.6725	9.4182	350	10/23/03	05/03/04	24	Mark L4-3D	B	2.03	1.41	1	1	+0.16
13	MER8	Merate	45.6725	9.4182	350	10/25/05	05/03/04	8	Episensor	B	-	-	-	-	-
14	MAR2	Marone	45.7397	10.1175	600	03/24/04	03/24/04	84	Trillium	A	1.49	1.76	1	1	+0.084
14	MAR0	Marone	45.7397	10.1175	600	03/24/03	03/24/04	73	Mark L4-3D	A	1.49	1.76	1	1	+0.084
14	M166	Marone	45.7397	10.1175	600	12/05/02	03/25/03	24	Mark L4-3D	A	1.49	1.76	1	1	+0.084
15	ASO2	Asolo	45.8049	11.9180	221	05/13/04	05/13/04	71	LE-3D/Lite	A	2.36	2.52	1	1	+0.12
15	ASOL	Asolo	45.8049	11.9180	221	03/04/03	05/13/04	76	Mark L4-3D	A	2.36	2.52	1	1	+0.12
16	NEGR	Negrar	45.4976	10.9482	167	06/29/04	05/13/04	43	LE-3D/5sec	A	1.21	1.57	0	0	-0.030
17	CTLE	Castelleone	45.2763	9.7622	66	09/21/04	05/13/04	22	LE-3D/5sec	C	1.21	2.10	0	0	-0.082
18	CORT	Cortemaggiore	44.9905	9.9075	52	06/30/04	10/08/04	14	LE-3D/5sec	C	-	-	0	0	-0.15
18	COR2	Cortemaggiore	44.9905	9.9076	52	05/26/05	06/23/05	13	Trillium	C	-	-	0	0	-0.15
19	PAVI	Pavia	45.2026	9.1349	82	06/12/05	06/12/05	18	Trillium	B	-	-	1	1	+0.58
19	PAV8	Pavia	45.2026	9.1349	82	06/12/05	06/12/05	18	Trillium	B	-	-	-	-	-
20	LAB2	Milano	45.4803	9.2321	125	05/30/05	05/30/05	25	Trillium	B	-	-	-	1	+0.48
20	LAB1	Milano	45.4803	9.2321	125	05/30/05	05/30/05	25	Episensor	B	-	-	-	1	-

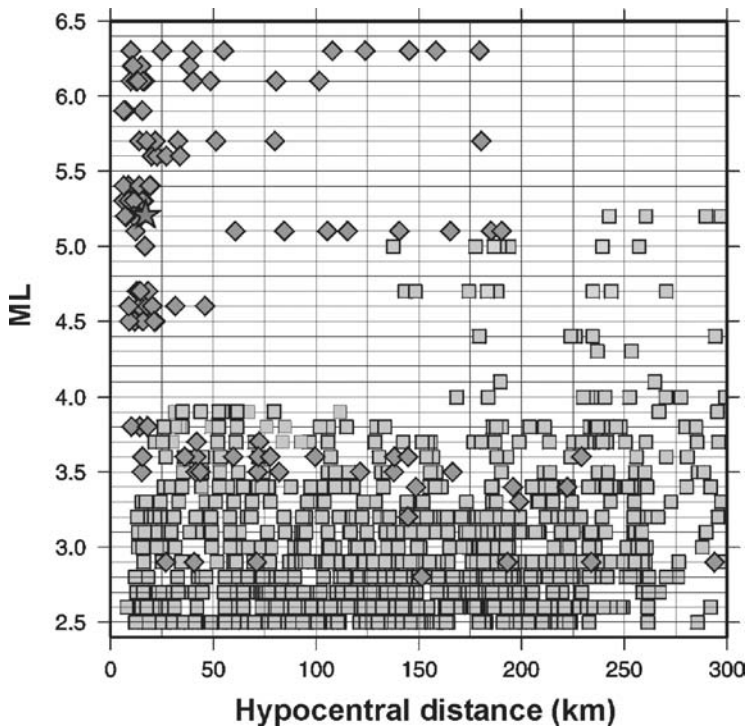


FIGURE 2 Distribution of earthquakes included in the INGV-MI data set versus hypocentral distance (light grey squares), for magnitude ranging from 2.5–5.2. The strong motions used as comparison (grey diamonds) are also reported. The gray star indicate the November 24, 2004 Salò earthquake (MI=5.2) recorded from the Gavardo RAN accelerometric station.

been differentiated and integrated. Both recorded and derived waveforms are then visually checked in order to avoid biasing peaks coming from both saturated signals and the application of analytical processes on the background noise. To check the reliability of the calculated peak ground accelerations, the recordings of stations LAB2 (Nanometrics Trillium 40 broadband sensor) and LAB1 (Kinematics-Episensor accelerometer), either located in the same site (station 19, see Table 1), have been analyzed: the derived acceleration values have been compared to those recorded by the accelerometer corrected for the instrumental response and band pass filtered in the same frequency range of the velocimeter [Frisenda *et al.*, 2005]. Finally, the accuracy of the results has been verified by overlapping real and derived seismograms (Fig. 3). The response spectra has been calculated for the component with the larger peak ground acceleration, using a standard damping of 5% [Bindi *et al.* 2006]; considering a cut-off pass band filter of 0.5 Hz, the analyzed periods (Table 3) range from 0.1 to 1.5 s [Boore and Bommer, 2005].

3. No Site Dependent Model

The general functional for modeling the attenuation of the ground motion, adopted in this study, is represented by the expression

$$\text{Log}_{10}(Y) = a + f_1(M) + f_2(R) \pm \sigma \quad (1)$$

TABLE 2 Available strong motion data used as comparisons

yyyy/mm/dd	hh:mm:ss	region	lat (°)	lon (°)	depth (km)	Ml	Source
1976/05/06	20:00:13	Eastern Alps	46.292	13.253	7.0	6.3	<i>Bragato and Slejko, 2005; Sabetta and Pugliese, 1987</i>
1976/05/07	00:23:49	Eastern Alps	46.245	13.269	9.0	5.0	<i>Bragato and Slejko, 2005</i>
1976/05/09	00:53:44	Eastern Alps	46.245	13.295	9.0	5.6	<i>Bragato and Slejko, 2005; Sabetta and Pugliese, 1987</i>
1976/05/11	22:44:01	Eastern Alps	46.258	12.985	6.0	5.3	<i>Bragato and Slejko, 2005; Sabetta and Pugliese, 1987</i>
1976/09/11	16:31:11	Eastern Alps	46.286	13.160	3.0	5.4	<i>Bragato and Slejko, 2005; Sabetta and Pugliese, 1987</i>
1976/09/11	16:35:03	Eastern Alps	46.277	13.175	12.0	5.7	<i>Bragato and Slejko, 2005; Sabetta and Pugliese, 1987</i>
1976/09/15	03:15:19	Eastern Alps	46.291	13.153	5.0	6.2	<i>Bragato and Slejko, 2005; Sabetta and Pugliese, 1987</i>
1976/09/15	09:21:19	Eastern Alps	46.318	13.119	8.0	6.1	<i>Bragato and Slejko, 2005; Sabetta and Pugliese, 1987</i>
1977/09/16	23:48:08	Eastern Alps	46.280	12.980	8.0	5.3	<i>Bragato and Slejko, 2005; Sabetta and Pugliese, 1987</i>
1979/09/10	21:35:00	Central Apennines	42.730	12.960	6.0	5.9	<i>Sabetta and Pugliese, 1987</i>
1984/04/29	05:02:03	Central Apennines	43.250	12.520	7.0	5.2	<i>Sabetta and Pugliese, 1987</i>
1998/04/12	10:55:32	Eastern Alps	46.324	13.678	15.2	5.7	<i>Bragato and Slejko, 2005</i>
2000/08/21	17:14:28	Western Po Plain	44.830	8.412	10.0	5.1	<i>Frisenda et al., 2005</i>
2002/02/14	03:18:02	Eastern Alps	46.426	13.100	11.2	5.1	<i>Bragato and Slejko, 2005</i>
2004/11/24	22:59:00	Northern Po Plain	45.670	10.540	10.0	5.2	<i>Pergalani et al., 2005</i>

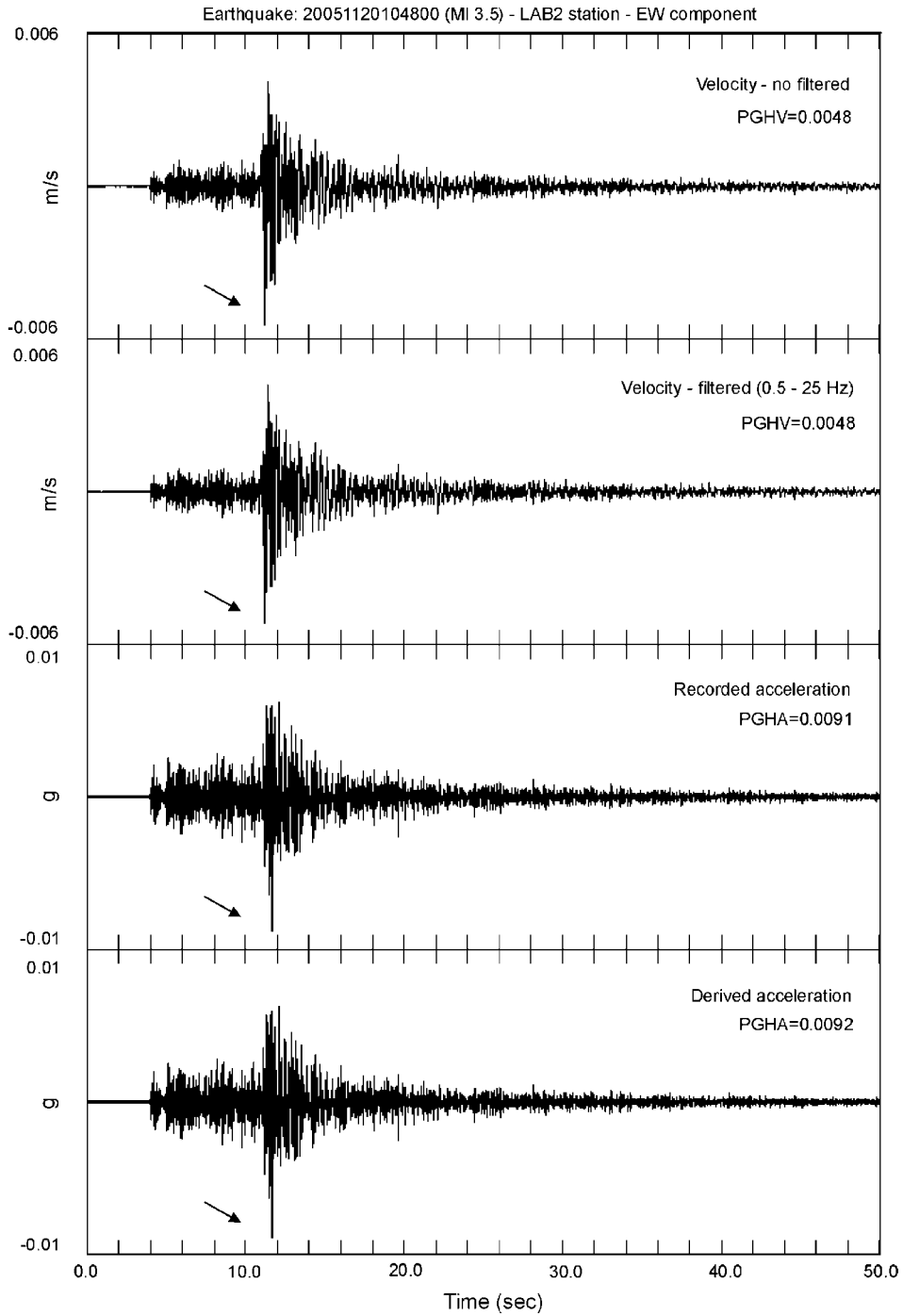


FIGURE 3 Examples of seismograms recorded from LAB2 velocimetric station and LAB1 accelerometric station, both installed in the same site. The recordings reported in this figure are related to the November 20, 2005 earthquake (MI=3.5).

TABLE 3 Regression coefficients for PGHA, PGHV, PGHD, and SA

equation	parameter	a	error	b	error	c	error	d1 stiff	d2 soft	σ
5	PGHA	-3.2176	± 0.17	0.7749	± 0.028	-1.7908	± 0.078	0.2560	-0.0854	± 0.312
5	PGHV	-4.1898	± 0.16	0.8778	± 0.026	-1.7211	± 0.071	0.2570	-0.0076	± 0.268
5	PGHD	-3.9542	± 0.16	0.9729	± 0.023	-1.6479	± 0.069	0.2460	0.0683	± 0.261
6	PGHA	-3.2191	± 0.16	0.7194	± 0.025	-1.7521	± 0.075	d soil 0.1780	-	± 0.282
6	PGHV	-4.1967	± 0.14	0.8561	± 0.022	-1.7270	± 0.065	0.1774	-	± 0.248
6	PGHD	-3.9474	± 0.14	1.0047	± 0.023	-1.7293	± 0.066	0.1726	-	± 0.232
6	SA - 0.1	-2.7799	± 0.14	0.6380	± 0.028	-1.7075	± 0.073	0.1254	-	± 0.351
6	SA - 0.3	-4.0539	± 0.11	0.8595	± 0.023	-1.5138	± 0.059	0.2338	-	± 0.261
6	SA - 0.5	-4.7976	± 0.11	0.9854	± 0.023	-1.5097	± 0.058	0.2259	-	± 0.274
6	SA - 0.7	-5.2896	± 0.12	0.9862	± 0.022	-1.4544	± 0.059	0.1936	-	± 0.271
6	SA - 0.9	-5.4916	± 0.12	0.9694	± 0.024	-1.4638	± 0.062	0.1342	-	± 0.268
6	SA - 1.1	-5.6916	± 0.11	1.0141	± 0.023	-1.5366	± 0.060	0.1332	-	± 0.264
6	SA - 1.3	-5.8083	± 0.11	1.0055	± 0.024	-1.5575	± 0.060	0.1430	-	± 0.263
6	SA - 1.5	-5.8847	± 0.12	0.9889	± 0.022	-1.5766	± 0.058	0.1547	-	± 0.259

where Y is the ground motion parameter to be predicted (PGHA value expressed in g, PGHV value expressed in m/s and PGHD value expressed in cm), $f_1(M)$ is a function of local magnitude, $f_2(R)$ is a function of distance, and σ is the standard deviation of the random variable $Log_{10}(Y)$. In this step, no terms which take into account the site geology have been introduced. Many forms of the functions in Eqn. (1) have been tested in the literature for many regions of the world [Sabetta and Pugliese 1996; Atkinson and Boore, 1997; Boore *et al.* 1997; Sadigh *et al.*, 1997; Ambraseys *et al.*, 2005a,b; Bragato and Slejko, 2005]. In this study, the coefficient a of Eqn. (1) represents the larger of the two horizontal peak values from an individual recording [Sabetta and Pugliese, 1987; Ambraseys *et al.*, 1996 a,b; Bindi *et al.*, 2006]. Other authors calculate the coefficient a both as the maximum value of the running vectorial composition of the horizontal time series [Bragato and Slejko, 2005] and as geometric mean of the two horizontal components (i.e., the mean of the logarithm, Campbell, 1997). In our case, some tests performed by using different approaches lead to obtain horizontal peak values characterized by no significant discrepancies; furthermore, such results demonstrate that the amplitude values relative to the horizontal components, such as considered in this article, are not affected by bias due to the orientation of the sensors installed in the field [Boore *et al.*, 2006]. Following several attenuation relationships performed starting from weak and strong motions occurred in the Italian regions in the last decades, the first function of Eqn. (1) has been implemented (in different times) both as

$$f_1(M) = (bM)$$

[e.g., Sabetta and Pugliese, 1987; 1996; Bindi *et al.*, 2006] and

$$f_1(M) = (bM) + (cM^2)$$

[e.g., Frisenda *et al.*, 2005; Bragato and Slejko, 2005]. In our case, the introduction in the source term of a further coefficient c does not allow us to improve the uncertainties of the process. Therefore, in the ground motion model a function $f_1(M)$ characterized by a constant magnitude scaling, with dY/dM equal to b , has been finally used.

In order to investigate the attenuation due to the geometrical spreading (geometrical attenuation) and to the material damping and scattering (anelastic attenuation), the propagation function $f_2(R)$ has been initially formulated as

$$f_2(R) = cLog_{10}(R) + dR$$

in which $cLog_{10}(R)$ represents the geometrical attenuation and dR represents the anelastic attenuation. As demonstrated in previous studies [e.g., Sabetta and Pugliese 1987; Frisenda *et al.* 2005], the anelastic coefficient d has not been found to be statistically significant, with a positive value very close to zero, so that it has been removed, and the propagation function has been reduced to $cLog_{10}(R)$. The proposed ground motion estimation equation is

$$Log_{10}(Y) = a + bM_L + cLog_{10}(R) \pm \sigma \quad (2)$$

where R , expressed in km, represents the hypocentral distance. Because the dimensions of the rupture surface for small events are usually smaller than the distances to

recording stations, the use of a hypocentral distance will not introduce significant bias into the attenuation relationships [Sadigh *et al.*, 1997].

Dissimilarly, in other studies the propagation term has been modelled as

$$c \text{Log}_{10} \sqrt{(R^2_{epi} + h^2)}. \quad (3)$$

In the case of data set characterized by high magnitude events recorded at distances of the order of the source dimension, h is a further parameter [Idriss, 1978; Campbell, 1981] to be estimated through regression; h is also introduced in the predicting model with the aim to incorporate all the factors (e.g., finite strength of the rock) that tend to limit the motion near the source, a property referred to as saturation with distance [McGuire, 1977; Joyner and Boore, 1981; Bolt and Abrahamson, 1982]. In our model, the introduction of a propagation term as reported in Eqn. (3) leads to relevant errors in the estimation of parameters h (both for PGHA, PGHV, and PGHD) with the result of a strong underestimation of the recorded data for distances lower than 50 km.

The regression of Eqn. (2) has finally been performed by the implementation of the nonlinear least-squares Marquardt-Levenberg algorithm [Press *et al.*, 1992] to determine the coefficients a , b , and c , without taking into account the site responses. The variable σ , representing the standard deviation of the random variable $\log_{10}(Y)$, has been obtained with a least square analysis. Considering the available data set, the use of different regression techniques (e.g., maximum likelihood approach) leads to very similar results. In many papers the dependence of the results with respect to the adopted regression methods has been demonstrated. Indeed, in cases of data set characterized by high values of magnitude ($M > 6.0$) and short distances (< 100 km) [e.g., Fukushima and Tanaka, 1990], an ordinary least squares analysis seems to lead, with respect to the use of the maximum likelihood approach, to biased results, underestimating the decay rate of the peak acceleration values with distance (higher coefficients “ c ” and lower coefficients “ b ,” Joyner and Boore, 1993).

4. Site-dependent Model

In order to take into account the local site effects, the ground motion model has been further developed through the introduction, by different approaches, of a function $f_3(S)$; thus, Eq. (1) can be re-written as

$$\text{Log}_{10}(Y) = a + f_1(M) + f_2(R) + f_3(S) \pm \sigma. \quad (4)$$

In order to evaluate the site responses, a first attempt has been performed by grouping the seismic stations in three soil categories (A, B, and C) following the classification reported in the EU8 code (after draft of May 2002, ENV, 2002):

- A. rock, V_s (i.e., mean propagation velocity within the first 30 m of depth and relative to the shear waves) > 800 m/s: Marine clay or other rocks (Lower Pleistocene and Pliocene), Volcanic rock and deposits (station number 3, 6, 7, 8, 9, 10, 11, 12, 14, 15, 16; see Table 1).
- B. stiff soil, $360 < V_s < 800$ m/s: Colluvial, alluvial, lacustrine, beach, fluvial terraces, glacial deposits, and clay (Middle-Upper Pleistocene). Sand and loose conglomerate (Pleistocene and Pliocene). Travertine (Pleistocene and Holocene) (station number 2, 4, 5, 13, 19, 20; see Table 1).

- C. soft soil, $V_s < 360$ m/s: Colluvial, alluvial, lacustrine, beach, and fluvial terraces deposits (Holocene) (station number 1, 17, 18, see Table 1). 245

The grouping of the stations into a particular class has been made following the results reported in Bordoni *et al.* [2003] in which, on the base of the geological information of the 1:500.000 Italian Geological Map, the Italian regions have been grouped into three classes A, B, and C according to EU8 provisions. In the area close to the seismic stations, the errors associated to the 1:500.000 scale have been checked by comparing this map with very detailed geological maps (scale 1:10.000 and 1:5.000). From such a comparison no significant differences has been observed. Following the EU8 code, 833 horizontal peaks recorded on rock, 163 horizontal peaks recorded on stiff soil, and 67 horizontal peaks recorded on soft soil have been obtained. In this case the function $f_3(S)$ assumes the form 255

$$f_3(S) = \sum_{i=1}^{N_d} d_i \text{class}(S, i)$$

where $\text{class}(S, i)$ is equal to 1 if site S is in class i and equal to 0 otherwise, N_d is the number of classes and d_i is a class coefficient to estimate through regression. Equation (2) can be re-written as

$$\text{Log}_{10}(Y) = a + bM_L + c\text{Log}(R) + d_1S_{stiff} + d_2S_{soft} \pm \sigma, \quad (5)$$

where S_{stiff} and S_{soft} are equal to 1 for stiff and soft soil, respectively, and 0 otherwise. The values of coefficients d_1 and d_2 have been determined by multiple nonlinear regressions: at each step the coefficients a , b , and c of Eq. (2) (both for PGHA, PGHV, and PGHD) have been obtained and then, repeating the process, the residuals have been used to estimate d_1 and d_2 , which in turn have been used to correct the values $\text{Log}_{10}(Y)$. In our case, it is worth noting that, both CTLE and CORT (same site of COR2, see Table 1) stations, installed in the core of the Po Plain and included in EU8 ‘‘C’’ soil category (Table 1), do not suffer amplification phenomena. As shown in the bottom right panel of Fig. 4, CTLE station (same results, not reported here, have been obtained for CORT station), located on very thick sedimentary formations (that exceeded 1,000 m) is characterized by negligible amplification factors (lower than 2) at frequencies lower than 1 Hz. Higher harmonics may be strongly damped by thick sedimentary covers [Prolai *et al.*, 2004]. Moreover, even in the presence of shallow sedimentary formations, the degree of stiffness, which characterized the sediments at local scale, can lead to obtain anomalous overestimation of V_{s30} values. The analysis of the regional data sets suggest that, although broad geologic classifications can be used to develop site factors for large regionally mixed data sets, individual recording sites can have site factors that significantly depart from these average trends [Campbell, 1989]. 265 270 275

Considering the remarks reported above, in order to carefully evaluate the site responses relative to our network, a simple but more objective NHV analysis has been computed. The microtremors recordings were processed by the Nakamura technique [Nakamura, 1989] taking into account signals recorded for each site in different noise conditions (both night and day). The signals were filtered by a band-pass filter ranging from 0.2–20 Hz and divided in time windows of 40 s. In this way it was possible to obtain statistical H/V spectral ratios in which the media and the standard deviation ($\pm 1\sigma$) have been 280

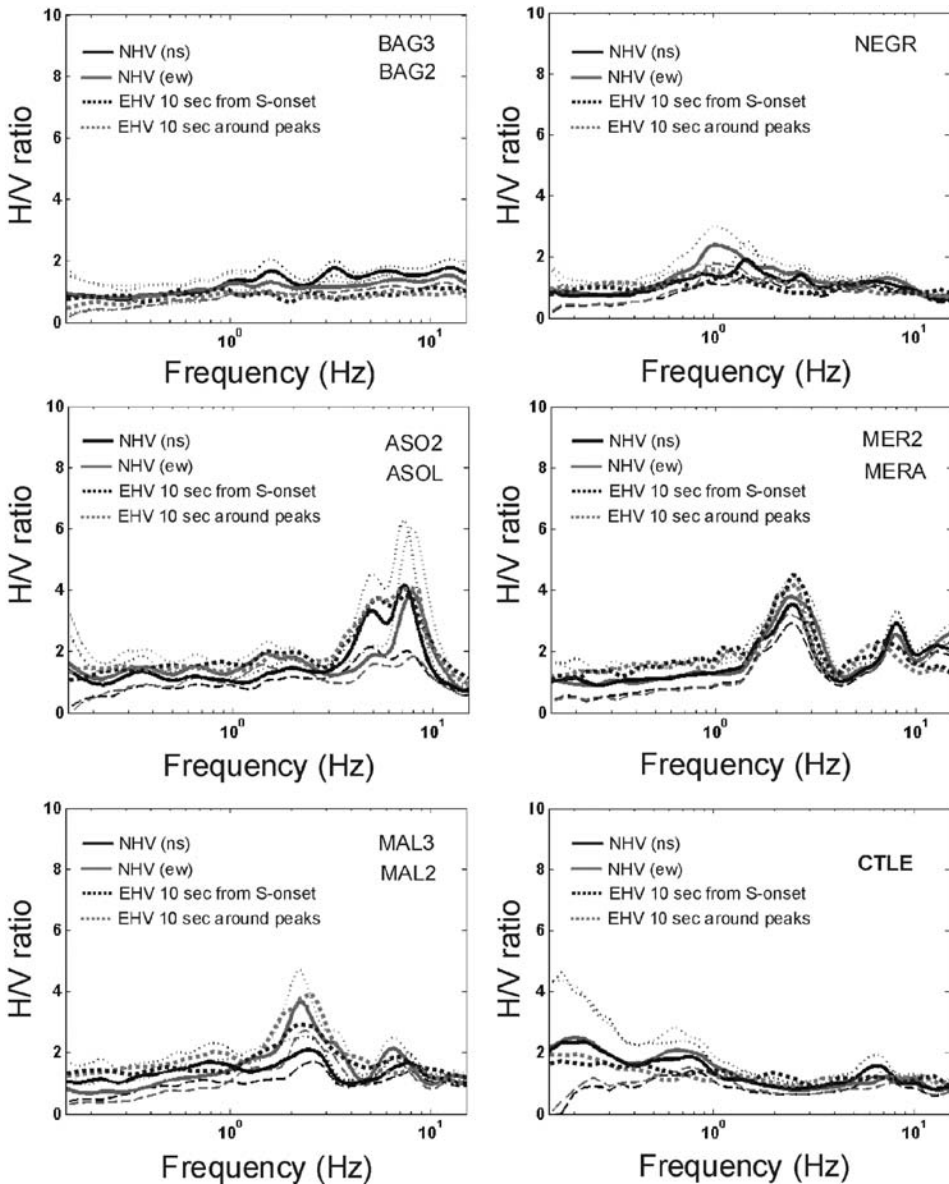


FIGURE 4 Examples of site responses calculated by Nakamura technique: the CTLE station is installed in the center of the Po Plain. Grey and black solid lines represent the mean of NS/Z and EW/Z, respectively, obtained averaging the results of spectral ratios calculated on a meaningful number of windows noise of 40 s; dashed and dotted lines represent \pm one standard deviation. For comparison, the results of EHV analysis are also reported: for each station solid and dashed black lines represent, respectively, the results of the H/V analysis (averaging the results derived by all available recordings and meaning the horizontal components) computed selecting, for each seismograms, both 10 s of window starting from the S-phase onset and 10 s of the S-phase window including the maximum horizontal peak.

computed (Fig. 4). In order to overcome the numerical instability that affects the H/V spectral ratios, an Hanning smoothing window has finally been applied [Press *et al.*, 285 1992]. Since many studies (i.e., Parolai *et al.*, 2004) show that Nakamura method is able to furnish reliable values of the dominant frequency of a site, even if in some cases it could underestimate the amplification factors, the results obtained by NHV have been compared to those coming from EHV. The Fourier spectra of seismic signals were computed considering time windows of 10 s (cosine tapering 10%) starting from the picking of the S 290 waves. In this case a band-pass filter ranging from 0.5–25 Hz, and an Hanning smoothing window with a half-width of 0.5 Hz has been applied. In the few cases in which the first 10 s of the S-phase did not include the recorded peak, the H/V spectral ratios have been re-calculated considering 10 s of signal surrounding the maximum horizontal value. In Fig. 4, it is possible to observe some examples of the convergence between the results obtained 295 calculating spectral ratios considering 10 s of seismic signals, selected starting both from the S-phase onset and from the surrounding of the maximum horizontal peaks.

In order to strengthen the results coming from both NHV and EHV, considering all seismograms recorded at each site, station magnitude residuals have been estimated. For each waveform recorded by a 3C station, zero to peak amplitude of synthetic Wood-Anderson 300 instruments have been calculated by convolving displacement signals (previously obtained by integrating velocimetric seismograms) with the standard Wood-Anderson torsion seismograph response. Station magnitudes for each recording have been computed without applying station corrections and averaging the horizontal components in a single measurement. For each station the mean magnitude residuals have been obtained comparing 305 single-station magnitude versus event magnitude and then averaging the results. As shown in the top panel of Fig. 5 and as reported in Table 1, the residuals confirm for each analyzed station the results of NHV analysis. It is worth noting as some stations included in class “A” of EU8 (e.g., MAL3 and in particular, ASO2) are characterized by positive values of station magnitude residuals (overestimation) and seem to show site effects in the 310 frequency range of interest (1–10 Hz), with amplification factor ranging between 3.5 and 4.5; on the contrary CTLE station, included in class “C” of EU8 shows both negative values of station magnitude residuals (underestimation) and absence of amplification phenomena. As already suggested in recent studies [Parolai *et al.*, 2004; Qamar *et al.*, 2003] differences in station magnitude can be directly related to different local site responses. 315

As final test the magnitude residuals have been compared to the station $LogY$ residuals (for PGHA, PGHV, and PGHD), calculated through a regression performed considering all horizontal peaks (1063 values for each $LogY$) and using the simple model reported in Eq. (2), without considering any site classification (Fig. 5, bottom panel). The agreement between the results of the analyses described above allows us to consider more reliable a site classification which distinguishes only rock sites and soil sites. In Table 1 for 320 each station the dummy soil coefficients are reported: coefficients equal to 0 indicate rock site in which the noise analysis give amplification factors lower than 2 for all considered frequencies. On the basis of NHV results, 422 horizontal peaks recorded on rock and 641 horizontal amplified peaks have been obtained. Then, Eq. (2) can be re-written as 325

$$Log_{10}(Y) = a + bM_L + cLog(R) + dS \pm \sigma \quad (6)$$

where S is equal to 1 for soil and 0 otherwise (see Table 1). The value of the coefficient d has been determined by a non-linear regression (LSQR algorithm; Paige and Saunders, 1982), starting from values of the coefficients a , b , and c previously estimated through the regression of 422 horizontal peaks (for PGHA, PGHV, and PGHD) recorded on rock. Also, for 330

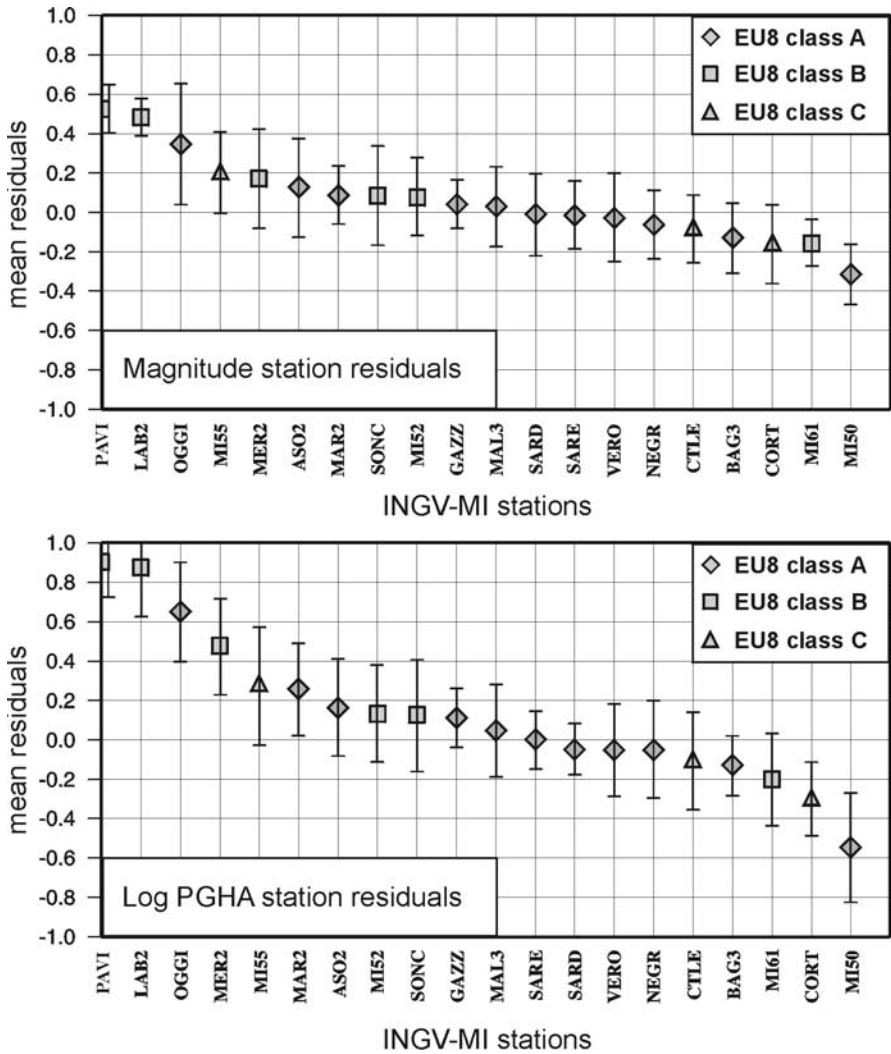


FIGURE 5 (Top panel) Mean station magnitude residuals; (bottom panel) Mean *Log-PGHA* residuals, calculated comparing, for each station, real data with respect to those obtained through a regression performed including all horizontal peaks (1,063 values for each *LogY*) and using the simple model reported in Eq. (2), without any site discrimination. The vertical bars represent the standard deviations. Similar results (agreement between magnitude and *LogY* residuals) have been obtained both for velocity and displacement.

“site dependent models,” the variable σ , representing the standard deviation of the random variable $\text{Log}_{10}(Y)$, has been obtained by a least square analysis.

In our case (i.e., agreement between the results coming from HV spectral ratios calculated both on seismic ambient noise and on local earthquakes; see Fig. 4), an evaluation of site responses based on spectral ratio calculated on microtremors, allows us to consider our models as predictive models for both rock and soil sites: indeed measurements of background noise recordings are cheap and quick to collect and spread the range of validity

of the proposed attenuation relationships for any site in which the estimation of ground shaking scenarios is necessary. It is worth noting that for estimating rock and soil site through a background noise analysis, the spectral ratio results coming from sensors installed near urban areas must always be carefully verified by computing the same analysis on earthquakes in order to avoid amplifications due to industrial plants and/or building free oscillations. The computed spectral ratios have been also used to test the method proposed by Bragato and Slejko [2005]. To detect the capability of this approach, the average H/V ratios in the interval 0.1–1.0 s has been computed for each station considering both Nakamura and receiver function techniques. For our dataset (see Table 1) the computation of the average H/V ratios over very large frequency intervals could lead to underestimating the real site amplifications by smoothing meaningful peaks. As an example, the Merate station (number 13 in Table 1), applying the Bragato and Slejko [2005] approach, appears as the second best site of our network, especially considering the average H/V ratios on receiver functions (1.41). On the contrary, as shown in Figs. 4 and 5, all receivers located in this site are characterized, with respect to the other stations that present greater values of the average H/V ratios (see sites number 6, 11, and 15 in Table 1), by signals that show non negligible amplification peaks at frequencies ranging from 2–3 Hz. This remark is in agreement both with magnitude and $\text{Log}_{10}(Y)$ residuals calculated for each station (Fig. 5).

5. Ground Motion Prediction Equations for Central-Northern Italy Earthquakes

Table 3 summarizes the coefficients obtained for Eqs. (5) and (6) described in the previous paragraph. The attenuation parameters have been estimated for PGHA, PGHV, PGHD, and SA by using hypocentral distances and local magnitudes calculated for each event included in the data set. For SA attenuation models, 8 periods ranging from 0.1–1.5 s have been considered. As shown in Table 3 (see σ values), Eq. (5), based on the EU8 soil classification, does not allow us, for all $\text{Log}_{10}(Y)$, to estimate d coefficients able to give models in agreement with the real data both for stiff and soft soils. Such a result, though it depends on the uneven representation of the soil classes in the data set (the small number of records collected by the stations included in the classes B and C of the EU8 code does not allow us to provide a reliable sampling of magnitude with respect to distance), is similar to that of previous studies [Ambraseys *et al.*, 1996 a,b; Lee and Anderson, 2000; Bragato and Slejko, 2005], which did not obtain any improvement of σ with the introduction of similar soil classification. Taking into account these remarks, in order to provide the most reliable attenuation relationships for the study area, Eq. (6) has been chosen as final models.

Figures 6a and 6b show the distribution of PGHA (expressed in g), PGHV (expressed in m/s), and PGHD (expressed in cm) values versus hypocentral distance (km), for different classes of local magnitude ranging from 2.5–5.2. Peak ground accelerations and peak ground displacements have been obtained by the procedure, described in the previous paragraphs, and applied to the horizontal components of velocimetric records. In the same figures the attenuation curves, obtained by the regression of Eq. (6), are plotted; for each magnitude range, the curves both for rock and soil data (solid and dotted gray lines) are reported. In the bottom left panel of Fig. 6b (grey star), it is possible to note the strong agreement between the real PGHA value (0.071 g, Pergalani *et al.*, 2005), related to the November 24, 2004 Salò earthquake ($M_l=5.2$) recorded by the RAN accelerometric station of Gavardo (located 14 km from the epicenter; hypocentral distance of 17 km), and the PGHA attenuation curve; the same consideration is valid for the PGHV value (0.032

(a)

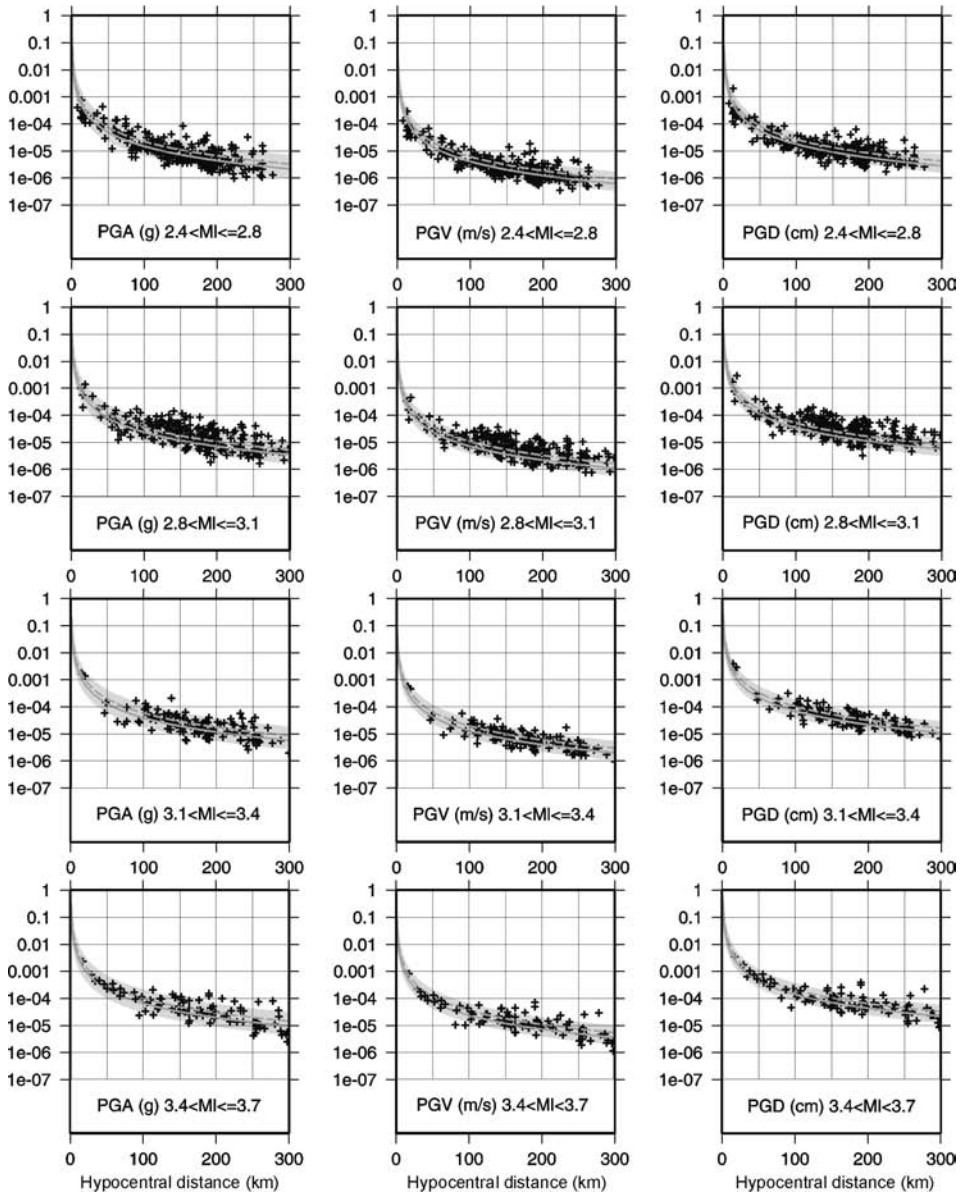


FIGURE 6 a) Plot of the attenuation curves (solid and dashed grey lines represent, respectively, the “no site dependent model” and the “site dependent model”), calculated for the events recorded by the INGV-MI stations, obtained inverting our PGHA (expressed in g) (left panels), PGHV (expressed in m/s) (central panels), and PGHD (expressed in cm) (right panels) data set and using Eq. (6) (the coefficient are reported in Table 3). For each panel the curves refer to the central magnitude value in the panel. The light grey strip represents the standard deviations. b) Same as Fig. 6a but for different classes of magnitude. Since there is a lack of high magnitude records, the data with M_I greater than 4.6 have been grouped. The grey stars reported in the bottom panels (for PGHA and PGHV) represent the peaks recorded by Gavardo accelerometric station.

(b)

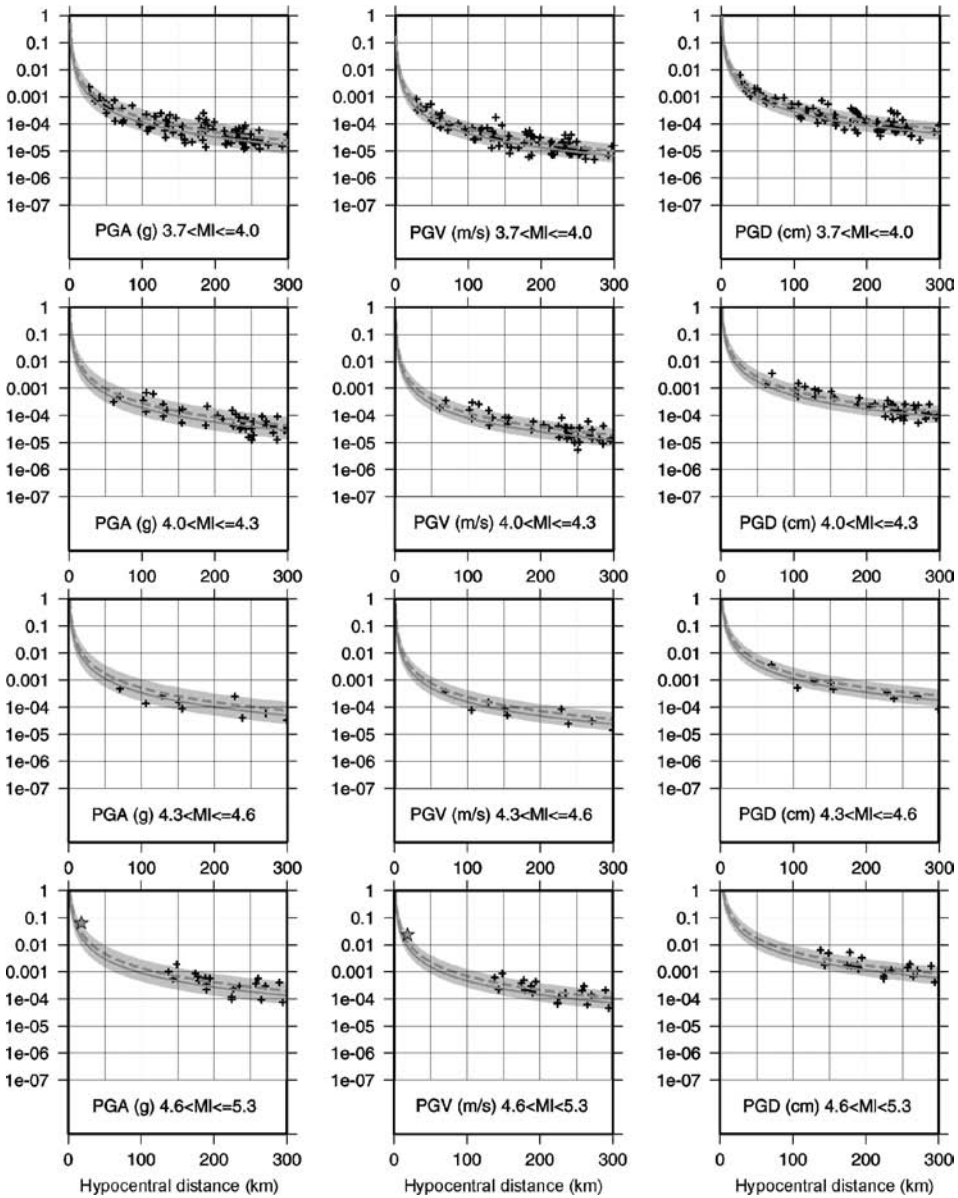


FIGURE 6 (Continued).

m/s, Pergalani *et al.*, 2005). Despite the lack of recordings in the near field, it is possible to observe that the distribution of the data shows seismic events with a local magnitude lower than 3.0 characterized by a strong decrease of peak values for distances up to 50 km. With respect to the relations calibrated for strong motions [Ambraseys *et al.*, 1996 a,b, 2005 a,b; Sabetta and Pugliese, 1987], the obtained attenuation models appear, in particular for the propagation term, more in agreement to other relations provided by using both weak and strong motions [Bragato and Slejko, 2005; Frisenda *et al.*, 2005]; it is worth

noting that both PGHA, PGHV, and PGHD models are characterized by geometrical 395
attenuation coefficients c higher than the unity, reflecting the great percentage of low
magnitude events included in the available data set. The values of coefficients b for the
magnitude term are higher than those obtained by Sabetta and Pugliese [1987], Ambraseys
et al. [1996 a,b, 2005 a,b] and most of the worldwide attenuation relationships derived for
magnitudes higher than 5.5 (b generally lower than 0.5); on the contrary, b values obtained 400
in this work reflect, as suggested both by Frisenda *et al.* [2005] and Bindi *et al.* [2006] for
ground models derived considering M_l up to 6.0, a strong dependence of PGHA, PGHV,
and PGHD on magnitude (even though for the displacement there are no relations for
comparison). In order to evaluate the distribution of residuals relative to Eq. (6) and its
central tendency the approach of Spudich *et al.* [1999] has been followed. The residuals 405
(for PGHA, PGHV, PGHD, and SA) are defined as the difference between the logarithms
of the observed and predicted values, and they are assumed to be normally distributed.
Spudich *et al.* [1999] defined the bias between observed and expected ground-motion
parameters as the mean value of the residual distribution; furthermore, they also character-
ized the residuals using basic variables such as the slope of the best fitting line through a 410
subset of residuals as a function of magnitude M or distance R (slope(M) and slope(R),
respectively). Bias and slopes obtained for PGHA, PGHV, and PGHD are shown in Fig. 7a:
for both local magnitude and hypocentral distance no significant trend is detected, with the
exception of a slight underestimation of predicted values for short distances and high

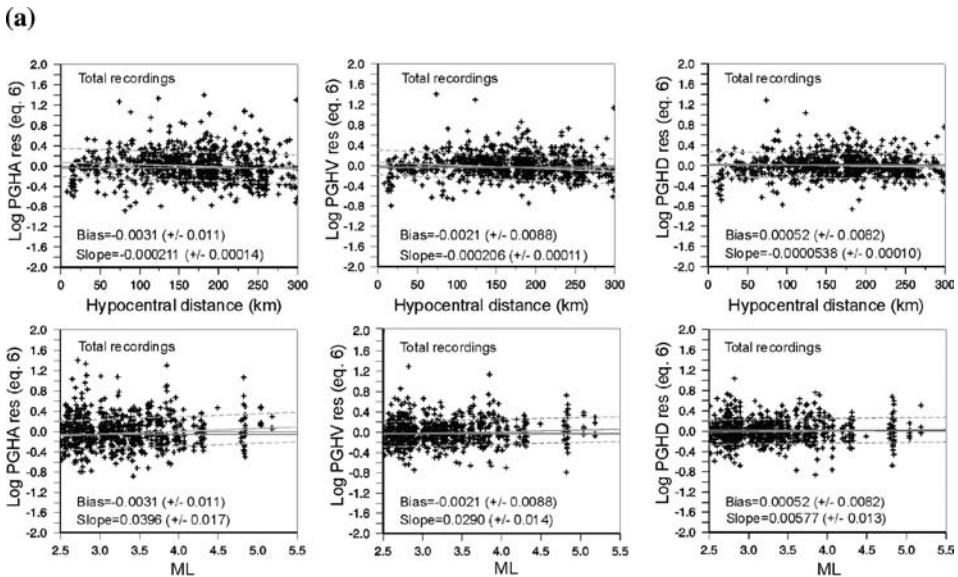


FIGURE 7 a) Residuals for PGHA, PGHV, and PGHD (logarithm for observations minus logarithm of predictions) estimated by the regressions performed considering Eq. (6) and calculated versus both local magnitude and hypocentral distance (considering both rock and soil recordings). Thick dark grey lines represent bias, light grey solid and dashed lines represent the residuals best fit and the standard deviations, respectively. b) Means (solid grey lines) and standard deviations (dashed grey lines) of PGHA (logarithm for observations minus logarithm of predictions) for different magnitude/distance classes. For each class the bias is also indicated (thick light grey solid lines).

(b)

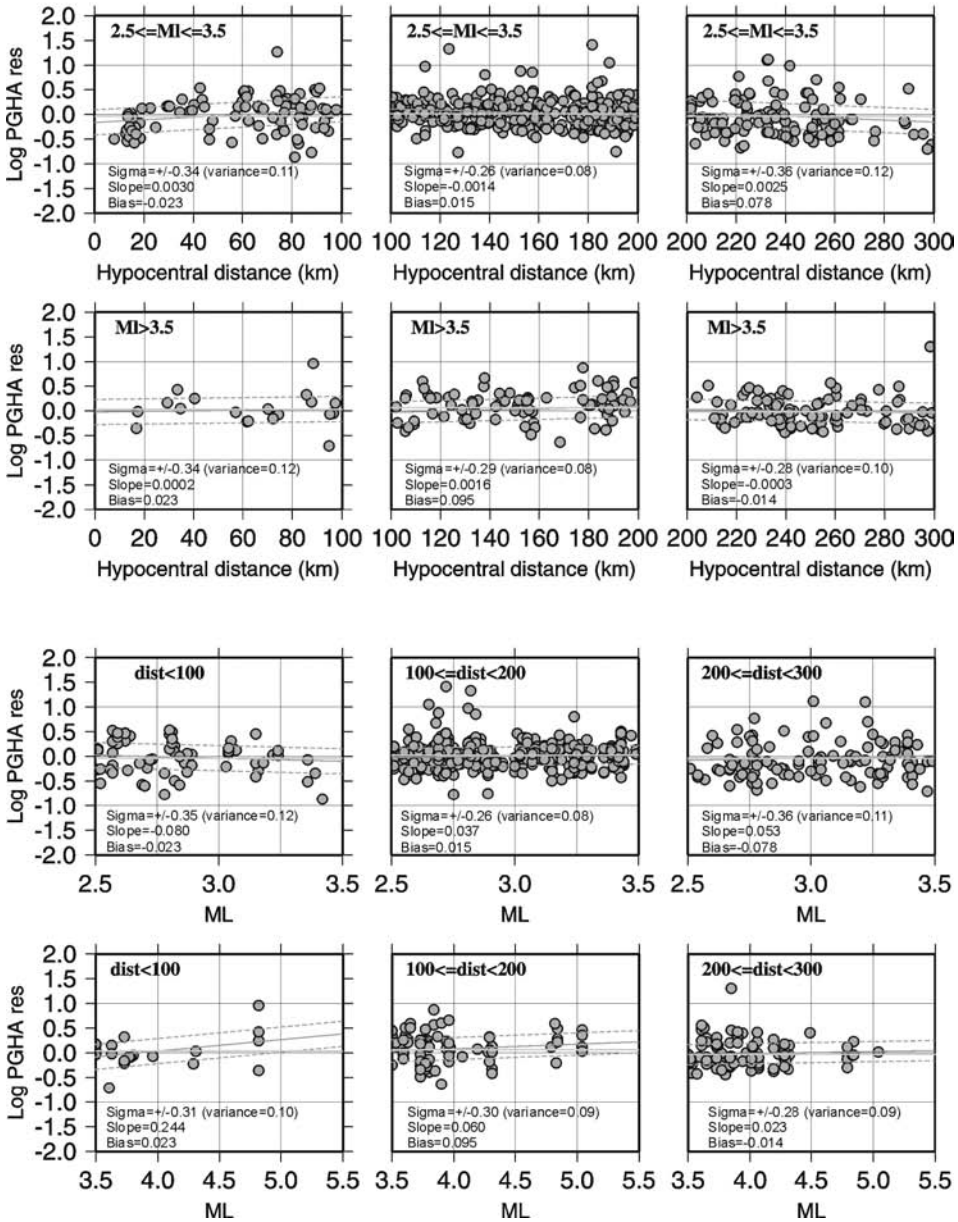


FIGURE 7 (Continued)

magnitudes. These results are confirmed by considering several sub-groups of data: the same computations have been performed in order to detect bias coming from a wrong coverage 415 of data in distance (for different magnitude values) and to check if the final results have been affected by possible effect of non-triggering stations [Bragato, 2004]. In Fig. 7b, the results obtained for Log_{10} PGHA residuals for different magnitude and distance classes are shown. Very similar results (not reported here) have been obtained both for PGHV and PGHD.

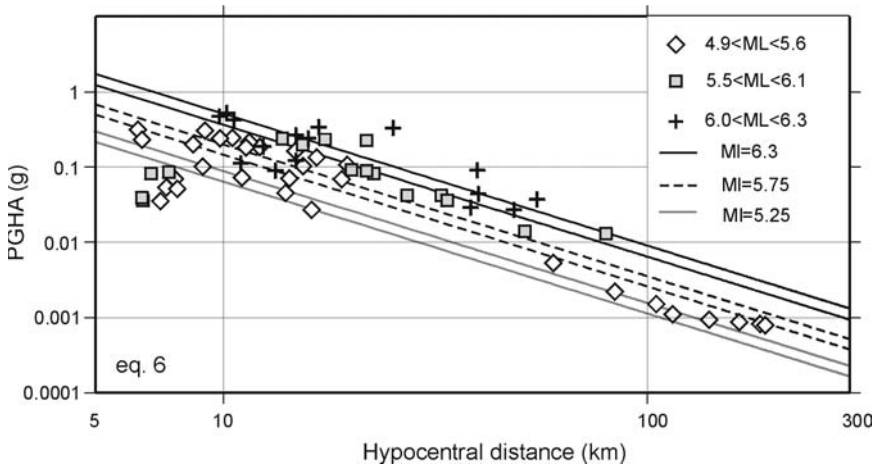


FIGURE 8 Comparison between PGHA attenuation curves obtained using Eq. (6) (for each magnitude the higher curve represents the “site-dependent” models), calculated for magnitudes 5.25, 5.75, and 6.3, and 69 PGHA related to the main strong seismic events occurred in North Central Italy in the last 30 years (see Table 2). For each event of Table 2, the hypocentral distances have been calculated.

No comparison with other empirical attenuation curves have been reported: at present, 420 predictive attenuation models for wide areas [Ambraseys *et al.*, 1996 a,b, 2005 a,b for European earthquakes; Sabetta and Pugliese, 1996, for Italian strong motions] have been estimated by using different independent variables (i.e., JB distance and/or epicentral distance). In Fig. 8, comparisons between 69 PGHA, relative to strong motions with MI ranging 425 from 5.0–6.3 (see Table 2) occurred in Central-Northern Italy in the last 30 years, and our PGHA attenuation curve, plotted for magnitude 5.25, 5.75, and 6.3, are shown. Although the attenuation models described by Eq. (6) must be considered predictive for the area ranging about from 8°30'E to 13°00'E and from 44°0'N to 46°30'N for earthquakes of MI up to 5.0 and for distances higher than 15 km, they are also able to provide, on the basis of the comparison shown in Fig. 8, reliable predictions both for higher MI (up to 6.0) and lower 430 distances (down to 10 km). For distances less than 5 km the model leads to incorrect results (no data are available); it is worth noting that in the near field the use of attenuation models presented in this study and in other studies are not able to take into account the non linear physical process in the neighborhood of the hypocentral area. Moreover, at present in Italy the lack of available accelerometric data recorded by trustworthy digital sensors at very short 435 distances (less than 10 km) represents an unsolved problem.

6. Conclusions

In this article, starting from a data set of 2,126 selected horizontal velocimetric records, attenuation relationships from Central-Northern Italy earthquakes have been defined. In 440 order to estimate the ground motion attenuation of the study area (Fig. 1), the regression procedures have been implemented in order to analyze acceleration, velocity, and displacement peak variations with respect to the local magnitude, hypocentral distance, and local site geology. The analyses have been performed by using seismic events with MI values ranging from 2.5–5.2. The attenuation relationships obtained for PGHA, PGHV, 445 PGHD, and SA, estimated both for rock and soil sites, are represented by Eq. (6) (Table 3).

The results in Figs. 6a and 6b show a strong agreement between empirical curves and both recorded (PGHV) and derived (PGHA and PGHD) data. The main conclusions of this study can be summarized as follows:

- Concerning attenuation relationships, the validity range is very important because it is very easy to overestimate or underestimate ground shaking parameters using the attenuation relationships without distinction. In this work the validity range of the predicted values (PGHA, PGHV, PGHD, and SA) is: local magnitude up to 5.0 and hypocentral distance less than 300 km. As it is shown in Figs. 7a and 7b, Eqs. 6 (see Table 3) can lead to an underestimation of the predictive values considering magnitude greater than 5.0 recorded at short distances. 450
- The ground motion predictive equations obtained in this article could represent a useful tool in the hazard assessment related to the most industrialized and populated areas of Italy. These regions, although are characterised by a poor rate of seismicity, represent areas potentially able to suffer energetic and harmful seismic events (e.g., the most recent is November 24, 2004 Salò earthquake, $M_l=5.2$ – damage of about 215 million euros); 460
- The reliability of attenuation models are strongly influenced by the level of accuracy in the estimation of soil coefficients; as demonstrated also in other works, soil classifications without accurate investigations performed at local scale (e.g., drillings, down-holes, bore-holes, seismic refraction tests), are not able to account for site effects (Table 3), leading to wrong results. Each region exhibited strong systematic differences in recorded accelerations at some sites that was not always related to obvious differences in surface geology. The results for specific recording sites demonstrate the complex nature of site response and clearly show the importance of including reliable site effects in the prediction of ground motion. Simple geologic classifications are believed to be appropriate for statistically characterizing site effects for relatively large, regionally mixed groups of recording sites; 470
- Since the distribution of records with respect to the EU8 classes (small number of records, in particular for class C) the available data set does not allow us to perform reliable regressions taking into account a subdivision of stations based on the EU8 code; in spite of this remark, the spectral analysis (in particular for the stations CTLE and CORT located in the center of the Po Plain) points out as such a classification can lead to wrong site response evaluations; 475
- The proposed sites discrimination based on background noise analyses allows us to perform a simple but more objective evaluation of site responses, leading to an increase of the quality of the results both in terms of fitting between real and predicted data and in term of standard deviation of the process (Figs. 6a, 6b; Table 3). Such a site discrimination allows us to satisfactorily sample the considered distance range (with respect to magnitude) both for rock and soil sites; 480
- Site coefficients evaluated from ambient noise measurements, fast and easy to collect, allow to spread the range of validity of the proposed attenuation relationships for any site in which the estimation of ground shaking scenarios is necessary. 485

References

- Ambraseys, N. N., Douglas, J., Sarma, S. K., and Smit, P. M. [2005a] “Equations for estimation of strong ground motions from shallow crustal earthquakes using data from Europe and the Middle East: horizontal peak ground acceleration and spectral acceleration,” *Bulletin of Earthquake Engineering* **3**, 1–53. 490

- Ambraseys, N. N., Douglas, J., Sarma, S. K., and Smit, P. M. [2005b] "Equations for estimation of strong ground motions from shallow crustal earthquakes using data from Europe and the Middle East: vertical peak ground acceleration and spectral acceleration," *Bulletin of Earthquake Engineering* **3**, 55–73. 495
- Ambraseys, N. N., Simpson, K. A., and Bommer, J. J. [1996a] "Prediction of horizontal response spectra in Europe," *Earthquake Engineering and Structural Dynamics* **25**, 371–400.
- Ambraseys, N. N. and Simpson, K. A. [1996b] "Prediction of vertical response spectra in Europe," *Earthquake Engineering and Structural Dynamics* **25**, 401–412. 500
- Atkinson, G. M. and Boore, D. M. [1997] "Some comparison between recent ground-motion relations," *Seismological Research Letters*, **68**, 24–40.
- Augliera, P., D'Alema, E., Marzorati, S., Bindi, D., Maistrello, M., and Gassi, A. [2004] "The 2003 data set of seismic waveforms recorded in Lombardia and Veneto regions (Northern Italy): site selection and MI scale calibration," *Abstracts of XXIX General Assembly of ESC*, Potsdam September 2004, 60. 505
- Bindi, D., Luzi, L., Pacor, F., Franceschina, G., and Castro, R. R. [2006] "Ground motion prediction from empirical attenuation relationships versus recorded data: the case of the 1997–98 Umbria-Marche (Central Italy) strong motion data-set," *Bulletin of the Seismological Society America*, in press. 510
- Bolt, B. A. and Abrahamson, N. A. [1982] "New attenuation relations for peak and expected accelerations of strong ground motion" *Bulletin of the Seismological Society America* **72**, 2307–2321.
- Bordoni P., De Rubeis V., Doumaz F., Luzi L., Margheriti L., Marra F., Moro M, Sorrentino D, and Tosi P. [2003] "Geological class map," in *terremoti probabili in Italia tra l'anno 2000 e 2030: elementi per la definizione di priorità degli interventi di riduzione del rischio sismico, Annex 1, Task 3.2*, 3–4 pp., GNDT Proj., Rome. 515
- Boore, D. M., Watson-Lamprey, J., and Abrahamson, A. [2006] "Orientation-independent measures of ground motion," *Bulletin of the Seismological Society America* **96**(4), 1502–1511.
- Boore, D. M. and Bommer, J. J. [2005] "Processing of strong-motion accelerograms: needs, options and consequences," *Soil Dynamics and Earthquake Engineering* **25**, 93–115. 520
- Boore, D. M., Joyner, W. B., and Fumal, T. E. [1997] "Equation for estimating horizontal response spectra and peak acceleration from Western North American earthquakes: a summary of recent works," *Seismological Research Letters* **68**(1), 128–153.
- Boore, D. M., Joyner, W. B., and Fumal, T. E. [1994] "Estimation of response spectra and peak accelerations from Western North American earthquakes, an interim report part 2," *U.S. Geological Survey Open File report*, 94–127. 525
- Boore, D. M., Joyner, W. B., and Fumal, T. E. [1993] "Estimation of response spectra and peak accelerations from Western North American earthquakes, an interim report," *U.S. Geological Survey Open File Report*, 93–509.
- Bragato, P. L. and Slejko, D. [2005] "Empirical ground-motion attenuation relations for the Eastern Alps in the magnitude range 2.5–6.3," *Bulletin of the Seismological Society America*, **95**(1), 252–276. 530
- Bragato, P. L. [2004] "Regression analysis with truncated samples and its application to ground-motion attenuation studies," *Bulletin of the Seismological Society America*, **94**(4), 1369–1378.
- Camassi, R. and Stucchi, M. [1996] "NT4.1, un catalogo parametrico di terremoti di area italiana al di sopra della soglia del danno (a parametric catalogue of damaging earthquakes in the Italian area)," CNR-GNDT, *Zincotecnica Nuova*, 66. 535
- Campbell, K. W. [1997] "Empirical near-source attenuation relationships for horizontal and vertical components of peak ground acceleration, peak ground velocity and pseudo-absolute acceleration response spectra," *Seismological Research Letters*, **68**(1), 154–180. 540
- Campbell, K. W. [1989] "The difference of peak horizontal acceleration on magnitude, distance, and site effects for small-magnitude earthquakes in California and eastern North America," *Bulletin of the Seismological Society America*, **79**, 1311–1341.
- Campbell, K. W. [1985] "Strong-motion attenuation relations: a ten year prospective," *Earthquake Spectra* **1**, 759–804. 545
- Campbell, K. W. [1981] "Near source attenuation of peak horizontal acceleration," *Bulletin of the Seismological Society America*, **71**, 2011–2038.

- Castro, R. R., Pacor, F., and Petru ngaro, C. [1993] "Confronto tra diversi metodi per la stima dell'attenuazione delle onde sismiche applicati nelle regioni Lombardia e Sicilia," *Atti XII Convegno, Consiglio Nazionale delle Ricerche, Gruppo Nazionale di Geofisica della Terra Solida*, 179–192. 550
- Cornell, C. A. [1968] "Engineering seismic risk analysis," *Bulletin of the Seismological Society of America* **58**, 1583–1606.
- Costa, G., Suhadolc, P., and Panza, G. F. [1998] "The Friuli (NE Italy) accelerometric network: analysis of low-magnitude high-quality digital accelerometric data for seismological and engineering applications," *Proc. Sixth U.S. National Conference on Earthquake Engineering*, May 31–June 4, published on CD-ROM, 435. 555
- Dost, B., Van Eck, T., and Haak, H. [2004] "Scaling of peak ground acceleration and peak ground velocity recorded in Netherlands," *Bollettino di Geofisica Teorica e Applicata* **43**(3), 153–168.
- ENV 1998, EUROCOD 8 [2002] "Design provisions for the earthquake resistance of structures. Seismic action and general requirements of structures," *CEN/TC 250, Draft*, May 2002. 560
- Frisenda, M., Massa, M., Spallarossa, D., Ferretti, G., and Eva, C. [2005] "Attenuation relationship for low magnitude earthquakes using standard seismometric records," *Journal of Earthquake Engineering*, **9**(1), 23–40.
- Fukushima Y. and Tanaka T. [1990] "A new attenuation relation for peak horizontal acceleration of strong earthquake ground motion in Japan," *Bulletin of the Seismological Society of America* **80**, 757–783. 565
- Gruppo di lavoro [2004] "Redazione della mappa di pericolosità sismica prevista dall'ordinanza PCM 3274 del 20 Marzo 2003," Rapporto conclusivo per il Dipartimento della Protezione Civile, INGV, Milano-Roma, 65.
- Idriss, I. M. [1978] "Characteristics of earthquake ground motions," *Proc. Of ASCE Speciality Conference on Earthquake Engineering and Soil Dynamics*, Pasadena, California, **3**, 1151–1265. 570
- Joyner, W. B. and Boore, D. M. [1993] "Methods for regression analysis of strong-motion data," *Bulletin of the Seismological Society of America* **83**(2), 469–487.
- Joyner, W. B. and Boore, D. M. [1981] "Peak horizontal acceleration and velocity from strong motion records including records from the 1979 Imperial Valley, California," *Bulletin of the Seismological Society of America* **71**, 2011–2038. 575
- Lee, W. B. and Anderson, J. G. [2000] "Potential for improving ground-motion relations in Southern California by incorporating various site parameters," *Bulletin of the Seismological Society of America* **90**(6b), 170–186.
- McGuire, R. K. [1977] "Seismic design spectra and mapping procedures relations," *Journal of Geotechnical Engineering Structural Dynamics* **5**, 211–234. 580
- Nakamura, Y. [1989] "A method for dynamic characteristics estimation of subsurface using microtremor on the ground surface," *Rep. Railway Tech. Res. Inst., Jpn*, **30**(1), 25–33.
- Paige, C. C. and Saunders, M. A. [1982] "LSQR: an algorithm for sparse linear equations and sparse least squares," *ACM Transactions on Mathematical Software*, **8**, 1. 585
- Parolai, S., Bindi, D., Baumbach, M., Grosser, H., Milkereit, C., Karakisa, S, and Zumbul, S. [2004] "Comparison of different site response technique using aftershocks of the 1999 Izmit earthquake," *Bulletin of the Seismological Society of America* **94**(3), 1096–1108.
- Pergalani, F., Compagnoni, M., and Petrini, V. [2005] "Confronti tra l'utilizzo di accelerogrammi generati e registrati nella valutazione dei fenomeni di amplificazione sismica in Lombardia," *Ingegneria Sismica*, Anno **XXII**(3), 36–51. 590
- Press, W., Teukolsky, S., Vetterling, W, and Flannery, B. [1992] *Numerical Recipes in C: The art of Scientific Computing*, Cambridge: Cambridge University.
- Qamar, A., Wright, A., and Thomas, G. [2003] "Using local magnitude scale to determine seismic site response in the Pacific Northwest," *Abstract, Eos. Trans. AGU*, **84** (46). 595
- Reiter, L. [1990] *Earthquake Hazard Analysis: Issues and Insight*, New York: Columbia University Press, p. 254.
- Sabetta, F. and Pugliese, A. [1996] "Estimation of response spectra and simulation of non-stationary earthquake ground motion," *Bulletin of the Seismological Society of America* **86**, 337–352.
- Sabetta, F. and Pugliese, A. [1987] "Attenuation of peak horizontal acceleration and velocity from Italian strong-motion records," *Bulletin of the Seismological Society of America* **77**, 1491–1513. 600

- Sadigh, K., Chang, C. Y., Egan, J. A., Makdisi, F., and Youngs, R. R. [1997] "Attenuation relationships for shallow crustal earthquakes based on California strong motion data," *Seismological Research Letters* **68**(1), 180–189.
- Spallarossa, D., Bindi, D., Augliera, P., and Cattaneo, M. [2002] "An MI scale in North-western Italy," *Bulletin of the Seismological Society of America* **92**, 2205–2216. 605
- Spudich, P., Joyner, W. B., Lindh, A. G., Boore, D. M., Margaris, B. M., and Fletcher, J. B. [1999] "SEA99: a revised ground motion prediction for use in extensional tectonic regimes," *Bulletin of the Seismological Society of America* **89**, 1156–1170.
- Suhadolc P. and Chiaruttini, C. [1987] "A theoretical study of the dependence of the peak ground acceleration on source and structure parameters," In: Erdik, M. and Toksoz, M., Eds. *Strong Ground Motion Seismology*, D. Reidel Publishing Company, 143–183. 610 1
- Theodulidis, N. P. [1998] "Peak ground acceleration attenuation of small earthquakes; analysis of Euroseist, Greece, data," The effects of surface geology on seismic motion; recent progress and new horizon on ESG study; *Irikura, Kudo, Okada and Sasatani (Editors)*. Rotterdam, Balkema. 615 2
- Toro, G. R., Abrahamson, N. A. and Schneider, J. F. [1997] "Model of strong ground motion from earthquake in Central and Eastern North America: best estimates and uncertainties," *Seismological Research Letters* **68**(1), 41–57. 3